Journal of the Serbian Chemical Society
JSCS-info@shd.org.rs • www.shd.org.rs/JSCS
J. Serb. Chem. Soc. 85 (11) 1383–1403 (2020) UDC 544.112:620.3:66.017+57+61:539.12
JSCS–5382 *Authors' review*

AUTHORS' REVIEW

From molecules to nanoparticles to functional materials

NENAD L. IGNJATOVIĆ[1], SMILJA MARKOVIĆ[1], DRAGANA JUGOVIĆ[1], VUK USKOKOVIĆ[2] and DRAGAN P. USKOKOVIĆ[1]*

[1]*Institute of Technical Sciences of the Serbian Academy of Sciences and Arts, Kneza Mihaila St. 35/IV, P.O. Box 377, 11000 Belgrade, Serbia and* [2]*Department of Mechanical and Aerospace Engineering, University of California Irvine, Engineering Gateway 4200, Irvine, 92697, CA, USA*

(Received 20 April, accepted 15 June 2020)

Abstract: Functional nanomaterials have held a steady position at the frontier of materials science and engineering in the 21st century. "Molecular Designing of Nanoparticles with Controlled Morphological and Physicochemical Characteristics and Functional Materials Based on Them" was the title of the research project funded by the Ministry of Education, Science and Technological Development of the Republic of Serbia and performed between 2011 and 2019 in the interdisciplinary area of nanoscience and nanotechnologies. Research activities within this program were divided into five interrelated topics: 1) from molecules to nanoparticles; 2) advanced ceramics with improved functional properties; 3) electrode materials for lithium–ion batteries; 4) nano-calcium phosphate in preventive and regenerative medicine; 5) biodegradable micro- and nano-particles for the controlled delivery of medicaments. This report gives an insight into this bibliographically most impactful Serbian national project on nanotechnologies executed within the aforementioned nine-year cycle, 2011–2019, focusing here only on the results achieved in the past three years. The project provided an outstanding and internationally recognized contribution to synthesis, characterization and functional design of a number of materials systems, including pure and lanthanide–doped hydroxyapatite, zinc oxides, sodium cobaltates, lithium iron pyrophosphates, lithium iron silicates and a number of polymeric systems.

Keywords: Bio-nano; electrodes; lithium-ion batteries; nanomedicine; nanotechnologies; review.

CONTENTS

* Corresponding author. E-mail: dragan.uskokovic@itn.sanu.ac.rs
https://doi.org/10.2298/JSC200426035I

1. INTRODUCTION

Advanced materials and nanotechnologies are of strategic importance for the developed and developing countries given that progress in them can help to address many social and technological challenges. Between 2011 and 2019, the Ministry of Education, Science and Technological Development of Serbia funded the project titled "Molecular designing of nanoparticles with controlled morphological and physicochemical characteristics and functional materials based on them" (MODENAFUNA, III–45004) within its Program of Integral and Interdisciplinary Research (PIIR III). Based on the current bibliographic data, with its 80 SCI articles, over 1500 citations and a Hirsch index of 23 as of the date the project closed, December 31, 2019, this project classifies as the most impactful out of the 18 other national projects on nanotechnologies funded within the same timeframe and all the PIIR III projects. More detailed bibliographic information is provided in the Supplementary material to this paper.

Even outside of the national boundaries, the importance of research realized within this project is at the very top of research in the field of nanomaterials. This research was focused on the discovery of fundamental and applicative knowledge in the molecular design of nanoparticles with predefined morphological and physicochemical characteristics and functional materials based on them. The main objective of this research was to acquire new knowledge and new technologies, which would be of benefit for science, technology and the whole society. One of the goals was also to improve experimental techniques, such as wet chemical synthesis with and without ultrasound field, mechano- and sono-chemical processing, hydro- and solvo-thermal processing, and various colloidal processing methods for obtaining hybrid nanocomposites. In other words, the goal was to enable the synthesis and the processing of various classes of nanoparticles and functional materials for the needs of a sustainable society (Fig. 1).

The results achieved in the first 6 years (2011–2016) are summarized in a previous authors review.[1] In the last three years (2016–2019), the project goals were realized in five interrelated topics: 1) from molecules to nanoparticles, 2) zinc oxide-based materials with enhanced functional properties, 3) energy storage materials, 4) nano-bio for preventive and regenerative medicine and 5) biodegradable micro- and nano-particles for the controlled delivery of medicaments.

This report is limited to the results achieved in the past three years (2016–2019) only.

Fig. 1. Global scheme of activities within the frame of the III 45004 MODENAFUNA project.

2. FROM MOLECULES TO NANOPARTICLES

A detailed analysis of the results achieved in the first 6 years (2011–2016) of the project is summarized in a previous publication.[1] Overall, the development of new bottom-up and top-down methods for the molecular design of nanoparticles allowed for the control the size, morphology and other physicochemical properties of different classes of inorganic, organic and hybrid nanoparticles (Fig. 2).

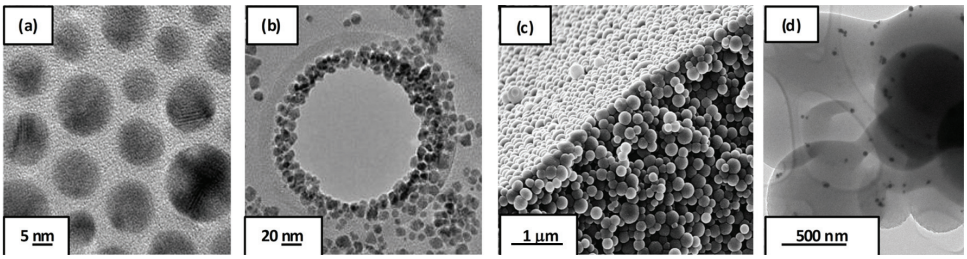

Fig. 2. The designed nanoparticles. a) TEM of gold nanoparticles, b) TEM of magnetic iron oxide nanocrystals, c) FESEM of PLGA/HAp/clindamycin nanospheres , d) FESEM of PLGA/AgNpPGA/ascorbic acid particles. (Reproduced with permission from the American Chemical Society and Elsevier).[2-5]

A simple and green solvothermal method was developed for the synthesis of monodisperse and spherical magnetic iron oxide nanoparticles of only 5 nm in

size and of gold nanoparticles of less than 10 nm in size, including various hybrid complexes based on them for application in different fields of biomedical engineering. A series of ZnO powders with different average particle sizes, morphologies and optical properties were prepared by hydrothermal and microwave processing and the powders exhibited pronounced antimicrobial activities. By controlling the nanoparticle size of Li-ion compounds and the type and the quantity of dopants and carbon distribution inside these composites, it was possible to optimize the electrochemical properties of these cathode materials. Various biodegradable multifunctional core–shell hydroxyapatite (HAp) – biodegradable polymer (poly-lactide-co-glycolide – PLGA, chitosan – Ch, chitosan oligolactate – ChOL, *etc.*) nanoparticles and other equally structurally sophisticated systems were created and their biological properties studied *in vitro* and *in vivo*. Novel procedures for the synthesis and the processing of nano–calcium phosphates suitable for hybridization with different biocompatible polymers and loaded with a variety of medicaments (vitamin D, antibiotics, *etc.*) were also developed for bone tissue engineering. Such systems are of particular interest in pharmacy and medicine, where the use of nanoparticles as carriers of medicaments allows for their delivery directly to the site of disease or injury.

Multimodal imaging (MI), a new and promising technique that could potentially improve the quality of diagnostic procedures while simultaneously saving time, requires completely new classes of multifunctional nanoparticles. MI attracted substantial attention due to the possibility of combining different modes of imaging, such as magnetic resonance imaging (MRI), computed tomography (CT) and photoluminescence (PL). For this purpose, new multimodal contrast agents based on nano–HAp doped with rare–earth (RE) ions were created.[6] Nanoparticles of gadolinium (Gd) doped HAp:Gd ($Ca_{4.775}Gd_{0.15}(PO_4)_3(OH)$) with magnetic properties were synthesized using emulsification and hydrothermal processing. The structure and the properties of HAp:Gd nanoparticles were further enhanced by co-doping with ytterbium (Yb), thulium (Tm) and europium (Eu). In addition to the magnetic properties, the particles of HAp:Gd,Yb/Tm ($Ca_{4.775}Gd_{0.03}Yb_{0.1}Tm_{0.02}(PO_4)_3(OH)$) also displayed photoluminescence by the upconversion mechanism. The luminescent properties were also exhibited by HAp:Gd,Eu ($Ca_{4.91}Gd_{0.02}Eu_{0.04}(PO_4)_3(OH)$) particles as well, but *via* the down-conversion mechanism (Fig. 3). X-Ray diffraction (XRD) and Rietveld refined plots confirmed the doping of the HAp structure with RE ions by the substitution of Ca^{2+} with Gd, Yb, Tm and Eu. All of the designed particles possessed a needle-like morphology. HAp:Gd,Yb/Tm particles emitted visible blue light upon the excitation at λ = 974 nm, while HAp:Gd,Eu particles emitted visible red light after e excitation at λ =370 nm. Both types of particles demonstrated good biocompatibility during *in vitro* assays with human dental pulp stem cell cultures.

Understanding the exact physicochemical transformations from atomic and molecular units suspended in the gaseous or the liquid state to desirable solid structures is foreseen as one of the grandest challenges for materials science in the decades that follow.[7] Most materials crystallize by passing through one or more of intermediate solid states, which may include polyatomic clusters, amorphous structures and various metastable crystalline polymorphs.[8]

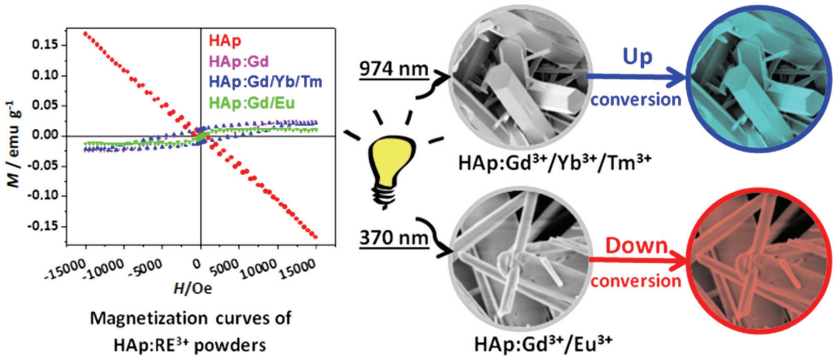

Fig. 3. Gd^{3+}, Yb^{3+}/Tm^{3+} and Eu^{3+} dual–doped HAp as magnetic, magnetic up-conversion and magnetic down-conversion materials.

One of the studies performed within this project fell within the scope of this aim.[9] It focused on understanding the kinetics of transformation of amorphous calcium phosphate (ACP) intermediates into different crystalline calcium phosphate compounds, including hydroxyapatite and α- and β-tricalcium phosphate. With the use of differential thermal analysis (DTA), the activation energies for the crystallization of ACP were calculated (Fig. 4) and it was deduced that structural water plays a key role in this transformation. The process of formation of needle-shape crystals of hydroxyapatite through the aggregation of ultrafine spherical units of ACP was followed on the nano scale and its mechanism was shown to involve 3D growth of preformed nuclei at high temperatures and edge--controlled nucleation under ambient conditions.

3. ZINC OXIDE-BASED MATERIALS WITH ENHANCED FUNCTIONAL PROPERTIES

Within the last four decades, zinc oxide–based materials have experienced growing interest in the materials science community because of the great possibilities that they offer. The attractiveness of ZnO lies in its wide bandgap energy at room temperature (3.37 eV), large exciton binding energy (60 meV), high electron mobility and transfer efficiency (115–155 $cm^2 \cdot V^{-1} \cdot s^{-1}$), intrinsic stability, non-toxicity, environmental compatibility, as well as the ease of their fabrication and cost-effective synthesis. Zinc oxide–based materials have been widely used in varistors, catalysts, spintronic devices, photodetectors, light emitting diodes, gas sensors, solar cells, energy storage and biomedical applications.

In the 21st century, when the energy crisis and environmental pollution have arisen as some of the major global problems, many efforts have been made by the materials scientists and engineers to develop solar light-driven photocatalysts efficient for both the removal of pollutants from water and photoelectrochemical (PEC) water splitting, yielding an efficient conversion of solar energy to chemical energy or electricity.

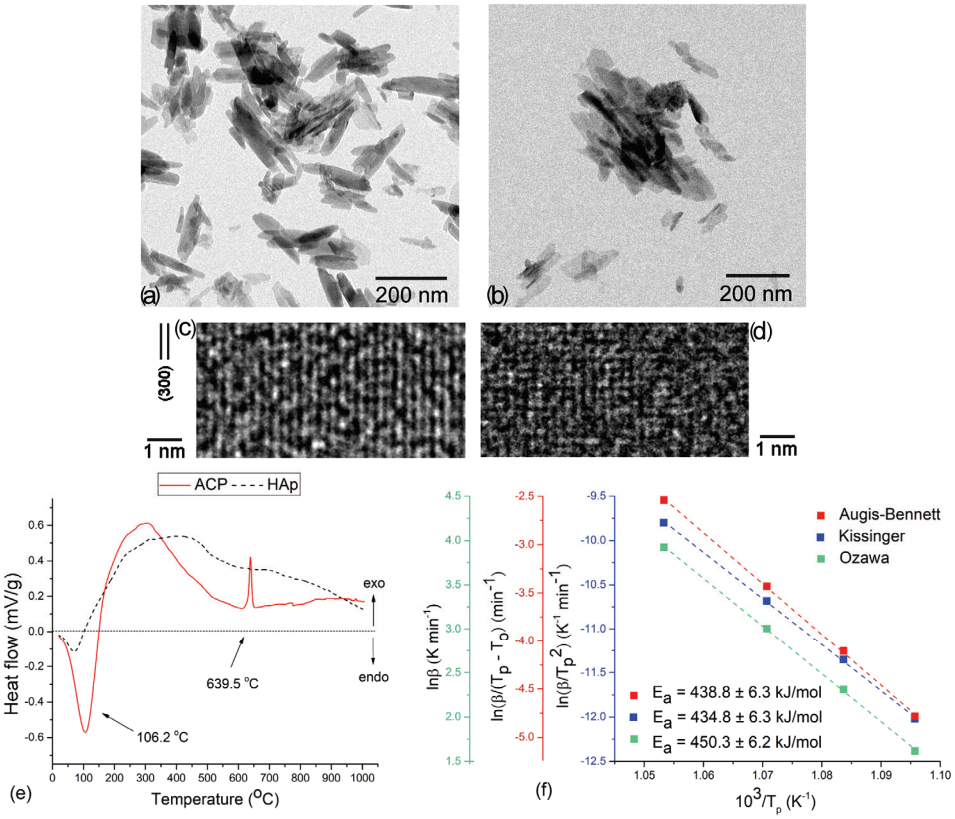

Fig. 4. TEM (a, b) and HR–TEM (c, d) images of crystalline (a, c) and amorphous (b, d) calcium phosphate nanoparticles at the nano (a, b) and atomic (c, d) scales. Differential thermal analysis diagrams (e) obtained by heating amorphous (ACP) and crystalline (HAp) calcium phosphate powders up to 1000 °C at a rate of 5 °C min^{-1}. Activation energies calculated for the crystallization reaction using the Kissinger, Augis-Bennett and Ozawa kinetic models (f). (Reproduced with the permission of the Royal Society of Chemistry).[9]

Zinc oxide has a great potential to be applied as a photo(electro)catalyst. With the band gap energy of 3.37 eV, this semiconductor can be activated only by UV light and it is an inefficient catalyst under the visible range of sunlight or indoor light irradiation. However, this drawback of ZnO as visible-light absorber

can be overcome by modifying the optical absorption properties of its particles. Over the years, in order to improve the visible light photocatalytic activity of ZnO materials, numerous approaches have been applied, such as: 1) metal and nonmetal ion doping, 2) hydrogenation, 3) incorporation of crystalline defects in the form of vacancies and interstitials, 4) modification of the particle morphology and surface topology, *etc.* Over the past three years, we successfully produced ZnO particles with improved functional properties by employing: 1) mechanical processing (of ZnO/SnO_2 heterojunction particles),[10] 2) microwave processing, 3) surface sensitization by polymers[11,12] and 4) partial substitution of zinc cations by iron cations.[13]

3.1. Mechanical processing

Mechanical activation of semiconductor powders enables the introduction of defects on the particle surface, which is important because surface defects reduce the recombination of photogenerated electrons and holes, thus enhancing the photocatalytic activity. Furthermore, the recombination of photogenerated electron–hole pairs can be efficiently reduced with the use of a heterojunction structure, that is, a combination of at least two semiconductors with different band gap energies, enabling better charge separation (Fig. 5a and b). Correspondingly, mechanical milling of ZnO and SnO_2 powders was employed to produce a ZnO/SnO_2 composite containing heterojunction particles and a high concentration of surface defects.[10] To determine the impact of surface defects on the photocatalytic activity, the relative concentration ratio of bulk-to-surface defects was modified by additional annealing of mechanically activated powder at 400 and 700 °C. The potential for application of a ZnO/SnO_2 composite as a photocatalyst was tested *via* de-colorization of methylene blue and degradation of phenol under direct sunlight irradiation. In both cases, the ZnO/SnO_2 composite particles exhibited enhanced photocatalytic activity as compared to bare ZnO. To comprehend the origin of the enhanced photocatalytic activity, a variety of characterization techniques were employed: XRD, Raman and Fourier transform infrared (FTIR) spectroscopy, field emission scanning electron microscopy (FESEM), laser diffraction particle size analysis, Brunauer–Emmett–Teller (BET) analysis, UV–Vis diffuse reflectance and photoluminescence spectroscopy, high-resolution transmission electron microscopy (HRTEM) and elemental mapping analyses. The FESEM analysis revealed that after 2 h of milling, no significant reduction of the ZnO particle sizes occurred, as their average size remained constant at about 120 nm. At the same time, the SnO_2 particles were noticeably modified, *i.e.*, after 2 h of milling, coarse polygonal grains with an average size of about 600 nm, organized in agglomerates of about 2 μm in size, were reduced to primary particles of 20 nm on average. The resulting ZnO/SnO_2 composite consisted of small spheroidal particles of tin oxide decorating the surface of larger

hexagonal ZnO submicron rods (Fig. 5c). Additional annealing at 400 and 700 °C slightly increased the particle size, as the particles started connecting by sintering.

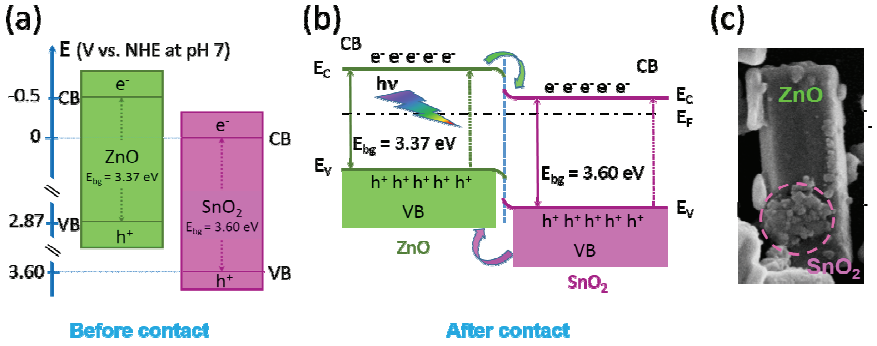

Fig. 5. Examples of the band structures for: a) semiconductors before contact and b) heterojunctions after semiconductors contact, along with c) an FESEM image of ZnO/SnO_2 hetero–particles obtained by mechanical milling.

Comprehensive results of the structural, morphological, textural and optical properties of the ZnO/SnO_2 composite and its elementary ingredients implicated a significant contribution of surface defects to the enhancement of the photocatalytic activity.

The high relative concentration ratio of surface–to–bulk defects was introduced by both milling and heterojunction interface effects. Surface defects adjusted the band gap, simultaneously increasing the capacity for visible light absorption as compared to the elementary ingredients of the composite. Surface defects, in particular zinc interstitials and oxygen vacancies, hindered the recombination of photogenerated electron–hole pairs as compared to `bare` ZnO. The annealing of the composite at 700 °C stimulated the diffusion of tin(IV) cations into the ZnO particles, leading to the formation of photocatalytically inactive Zn_2SnO_4 and bulk oxygen vacancies, which acted as recombination centres for the charge carriers, resulting in loss of photoactivity.

3.2. Microwave processing

During research on ZnO, it was found that microwave (MW) processing can have profound effects on the functional properties of ZnO materials. This is explained by the fast crystallization of nanostructured particles generated by the MW energy, which enables the introduction of both bulk and surface defects.[11] Since it is known that bulk defects can act as recombination centres that deteriorate the photocatalytic activity of the material, the influence of point defects, especially the surface-to-bulk defects ratio, on the crystal structure and the optical and photo(electro)catalytic properties of MW-processed ZnO particles were studied. First, the concentration and the type of point defects on the surface of MW-pro-

cessed ZnO particles were varied *via* surface sensitization by polyethylene oxide (PEO) with different molecular weights (200, 600 and 900 kg·mol^{-1}).[11] It was shown that PEO acts as a source of oxygen interstitials on the surface of ZnO particles, which have a profound effect on the direct absorption of sunlight, simultaneously enhancing the photodegradation of methylene blue.

More recently, the surface-to-bulk defects ratio in ZnO particles was modified using surfactant-directed MW processing and two types of surfactants: cetyltrimethylammonium bromide (CTAB, $C_{19}H_{42}BrN$) as a cationic surfactant and Pluronic F127 ($EO_{106}PO_{70}EO_{106}$) as a nonionic one.[12] To correlate the surface-to-bulk defect ratio with charge separation and radiative recombination of photogenerated electron–hole pairs, the crystal structure and the morphological, textural, optical and photo(electro)catalytic properties of the processed ZnO particles were examined in detail. It was found that a small amount of surfactant (5 wt. % of CTAB or Pluronic F127 with respect to $ZnCl_2$) was needed to allow for tuning of the nanocrystallite polarity, particle texture and morphology, and the surface-to-bulk defects ratio. The impact of the surfactants on the surface-to-bulk defects ratio was confirmed by the relationship between the intensities of the E_{2H} mode and the A_1 (LO) + E_1 (LO) mode in the Raman spectra, which is illustrated in Fig. 6a. An increase of the $E_{2H}/(A_1\ (LO) + E_1\ (LO))$ intensity ratio confirmed the decrease of the concentration of intrinsic lattice defects with the addition of either surfactant. The decreased amount of oxygen vacancies in the crystal lattices of ZnO/CTAB and ZnO/F127 compared to bare ZnO was attributed to the *in situ* action of the polymers as passivating agents.[12] The bromide anions of CTAB or oxygen ions of Pluronic can fill up the singly (V_O^+) or doubly (V_O^{++}) charged states of oxygen vacancies in the ZnO lattice. The results of the Raman spectroscopy measurements were supported by the results of the photoluminescence spectroscopy (Fig. 6b).

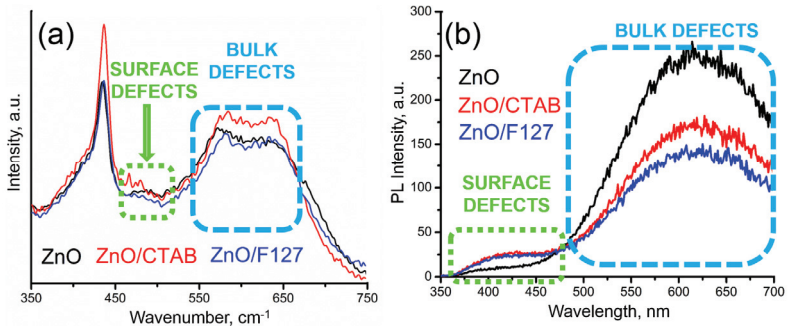

Fig. 6. a) Raman and b) photoluminescence spectra of microwave-processed ZnO particles.

The synergy of all of the abovementioned properties, namely the nanocrystallite polarity, particle texture and morphology, and the surface-to-bulk defects

ratio resulted in enhanced optical and photo(electro)catalytic properties of the ZnO particles. The best photo(electro)catalytic properties were exhibited by the ZnO/CTAB sample. After 2 h under direct sunlight illumination, ZnO/CTAB decolorized 10 ppm methylene blue dye water solution with 100 % efficiency and with a decolourization halftime of 26.4 min. In addition, ZnO/CTAB exhibited excellent properties as a photoanode. When the ZnO/CTAB photoanode was illuminated with 90 $mW \cdot cm^{-2}$, the current density measured at 1.5 V *vs*. saturated calomel electrode (SCE) reached 27.0 $mA \cdot g^{-1}$. Illumination of the ZnO/CTAB photoanode induced a significant shift of the overpotential toward lower values, to be exact from 1.296 to 0.248 V *vs*. SCE. The ZnO/CTAB photoanode showed 1.9- and 1.5-fold higher photoresponse than ZnO and ZnO/F127, respectively. The ZnO/CTAB photoanode provided efficient charge transfer across the electrode/electrolyte interface, with a longer lifetime of the photogenerated electron–hole pairs and reduced possibility of charge recombination. The fastest charge transfer of electrons across the electrode/electrolyte interface occurred when ZnO/CTAB was used as the photoanode. The photoconversion efficiency of ZnO/CTAB was 4.2 %. Complete analyses revealed that the optimal surface-to-bulk defects ratio was favourable for improvement of the photo(electro)catalytic properties.

In our latest study on ZnO with enhanced functional properties, the effect of zinc-to-iron cation substitution on the local structure, defect formation, and hyperfine interactions in MW-processed $Zn_{1-x}Fe_xO$ (x = 0, 0.05, 0.10, 0.15 and 0.20) nanoparticles was assessed.[13] Mössbauer spectroscopy measurements and the first–principles calculations of hyperfine interaction parameters were used to study the local structure and defects formation in $Zn_{1-x}Fe_xO$ particles. Evidence concerning the crystallite size, the particle morphology and magnetic properties was obtained using XRD, TEM and SQUID magnetometry, respectively. Mössbauer spectroscopy measurements revealed that all the iron cations in the $Zn_{1-x}Fe_xO$ particles were trivalent. More precisely, Fe^{3+} substituted Zn^{2+} in the $Zn_{1-x}Fe_xO$ crystal structure, with Zn vacancies being in the nearest neighbour environment, and these results were in agreement with the first–principles calculations. The magnetic measurements indicated that MW processing provided a random distribution of Fe^{3+} in the ZnO host lattice without any accumulation, except for the sample with 20 at. % Fe, where these dopant ions segregated into an impurity phase. This study revealed that MW processing introduces a large number of vacancies, which facilitate the creation of Fe^{3+}–V_{Zn} pairs.

This overview of our recent results indicates that an enhanced photocatalytic activity of ZnO-based materials can be achieved by: 1) mechanical activation of ZnO powder due to the introduction of surface defects,[10] 2) mechanical processing of ZnO/SnO_2 composite due to the synergetic effect of the surface defects and the ZnO/SnO_2 heterojunction particles, which both facilitate charge separ-

ation, thereby hindering recombination of photogenerated carriers,[10] 3) microwave processing due to the introduction of both surface and bulk defects,[11] 4) *in situ* use of surfactants due to their enabling tuning of the surface-to-bulk defects ratio.[12]

4. ENERGY STORAGE MATERIALS

A significant part of the project was dedicated to investigation of several compounds as potential electrode materials for Li/Na rechargeable batteries. In particular, the research aimed at correlating the structural and morphological properties of the synthesized materials with their electrochemical properties. Both the easiness and the cost of the synthesis were key criteria in selecting materials and methods for these correlations.

TiO_2 nanotube arrays grown on Ti foils present concurrently current collectors and anode materials, a combination of properties that is promising for the new generation of ultrathin lithium-ion batteries. Anatase nanotube arrays were grown by anodic oxidation of titanium foils for 6 h in a 0.7 % solution of NH_4F in glycerol, under the voltages of 20, 30, 45 and 60 V, followed by annealing for 3 h at 400 °C in air.[14] This temperature was sufficient to induce the crystallization of the anatase phase of TiO_2. The inner diameter of the nanotubes was proportional to the applied voltage, while their thickness was independent of it. At 20 V, the diameter was around 60 nm and it increased to 110–140 nm when a voltage of 45 V was applied. Interestingly, the mean crystallite size was largest at the lowest applied voltage and it slowly decreased with increasing applied voltage. Cyclic voltammetry experiments showed that both insertion and extraction of lithium ions are diffusion-controlled. Galvanostatic experiments confirmed that the charging capacity increased with the surface-to-volume ratio, in which sense the anatase nanotube arrays behaved similarly to the behaviour of very small nanoparticles described in the literature. A capacity fade during discharge was observed only for nanotubes obtained at the highest anodization voltage.

Li_2FeSiO_4 has the potential to extract more than one lithium ion per transition metal ion, which is beneficial for both the charge capacity and the energy density. Within the several polymorph structures that could occur, the lithium, iron and silicon ions are positioned at the tetrahedral sites of the monoclinic structure with $P2_1/n$ symmetry (Fig. 7). In particular, lithium ions occupy two different tetrahedral positions, which are usually denoted as L1 and L2, while iron ions take one tetrahedral position.[15] Combined XRD and DFT studies were performed to examine the previously observed antisite defect, where lithium and iron ions exchange their positions. A solid-state reaction method was used for the synthesis of Li_2FeSiO_4 samples and the crystal structure refinement confirmed the presence of 6 at. % of antisite defects. Based on density functional theory (DFT) calculations, iron replaced lithium exclusively in one position, *i.e.*, the L2

site. Namely, the Fe–Li2 antisite appeared to be energetically favourable compared to the Fe–Li1 antisite defect and to pristine, that is, the antisite defect-free structure. The formation of the Fe–Li2 antisite is governed by both electronic and geometrical relaxations.

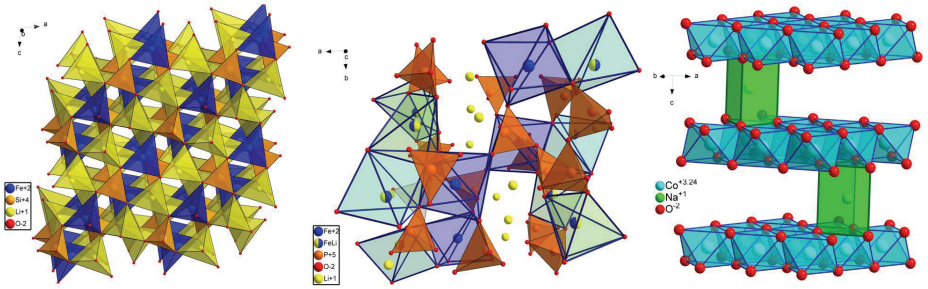

Fig. 7. The structures of Li_2FeSiO_4, $Li_2FeP_2O_7$ and Na_xCoO_2 from left to right, respectively.

Lithium–iron(II) pyrophosphate ($Li_2FeP_2O_7$) is a compound that also has two lithium ions per transition metal ion and possesses a somewhat higher voltage *vs*. Li/Li+. $Li_2FeP_2O_7$ was synthesized by precipitation from aqueous solutions of $LiNO_3$, $FeSO_4$ and $(NH_4)_2HPO_4$ mixed in this order.[16] A new method was developed for the synthesis of composite $Li_2FeP_2O_7$/carbon powders that utilized soluble methylcellulose as both a dispersing agent and a carbon source. XRD confirmed the presence of $Li_2FeP_2O_7$ as the major phase and also the olivine-type $LiFePO_4$ as a minor phase in amounts of around 9 wt. %. Crystal structure refinements were realized in $P2_1/n$ and *Pnma* space groups for $Li_2FeP_2O_7$ and $LiFePO_4$, respectively. The structure of $Li_2FeP_2O_7$ was shown to contain three different crystallographic positions fully occupied by lithium ions, one position fully occupied by iron ions, and two different crystallographic positions that are partially occupied by both lithium and iron ions (Fig. 7). The results of the refinement procedure combined with the results of Mössbauer spectroscopy revealed a difference in the partial occupancy of the mixed–occupied sites by lithium ions. It was proposed that the more reductive atmosphere attained during the pyrolysis of methylcellulose was the cause of the altered partial occupancy that could affect lithium diffusion. In addition, *in situ* formation of carbon enabled the reduction of the crystallite size. Electrochemical measurements recorded markedly higher charge/discharge capacities in the composite powder. The profile of the discharge curves in both cases changed from a gentle slope from 4 to 3.4 V to a plateau at 3.4 V to steeper slop at the end of the curve, with the plateau originating from the $LiFePO_4$ olivine phase. Electrochemical impedance spectroscopy revealed a significantly lower charge-transfer resistance and a slightly higher Warburg impedance for the $Li_2FeP_2O_7$/C electrode. This means that the more conductive network attained in the composite powder facilitated electron transfer,

while the smaller crystallite size shortened the diffusion length of the lithium ions. Apparently, different partial occupancies of the mixed-occupied sites had no influence on the improvement of the cycling behaviour.

Previous research demonstrated the enhancement of the electrochemical properties of $LiFePO_4$ on fluorine doping.[17,18] Considering this, the follow-up research aimed at investigating for the first time the influence of fluorine doping on the structure, and magnetic and electrochemical properties of layered Na_xCoO_2.[19] Na_xCoO_2 crystallizes in several layered structures denoted as O3, P2 and P3. They are characterized by the edge-sharing CoO_6 octahedra in the form of $(CoO_2)_n$ sheets between which are sodium ions in prismatic or octahedral coordination. The P2 type of structure is considered to be the most suitable for energy storage applications (Fig. 6). Na_xCoO_2 ($x \approx 0.75$) was synthesized by a solid-state reaction between Na_2CO_3 and Co_3O_4 through a method that included sequential cycles of rapid heating to 750 °C in air, a dwell time of 15 min and rapid cooling to room temperature. It turned out that the synthesis of fluorine-doped Na_xCoO_2 (NCOF) was not a trivial task and after several failed attempts, a vapour–solid reaction between NH_4HF_2 and pristine Na_xCoO_2 proved itself to be a successful approach. The morphologies of the synthesized powders were similar, showing polyhedral, highly agglomerated particles. The syntheses were followed by XRD measurements and the diffractometric patterns of the fluorinated powders showed the presence of Na_xCoO_2 as the major phase and about 2.8 wt. % of NaF. Peak broadening effects were also observed, along with a significant shift of both the diffraction maxima and their relative intensity ratios. The crystal structure of both powders were refined in the $P6_3/mmc$ space group, with the caveat that only the z coordinate of the oxygen site could be refined since sodium and cobalt ions were in special positions. Fluorine ions, in turn, were free to occupy the oxygen sites. The fluorination caused a decrease of the Na/Co atomic ratio (from 0.76 to 0.44), a small decrease of the lattice parameter a, an increase of the lattice parameter c, a reduction of the crystallite size, a decrease of the NaO_2 interslab thickness, and an increase of the CoO_2 slab thickness. These findings implied that apart from the extraction of sodium ions from the lattice, fluorination enabled the incorporation of fluorine into the lattice, thus modifying the average oxidation state of cobalt. X-Ray photoelectron spectroscopy results confirmed these findings. Namely, upon fluorination, the average oxidation state for cobalt increased from 3.24 to 3.52; combined with sodium occupancies obtained by the refinement, this led to the deduction of $Na_{0.76}CoO_2$ and $Na_{0.44}CoO_{1.96}F_{0.04}$ as the compositions of the pristine and the fluorinated phases, respectively. Magnetization measurements showed that fluorination modified the spin system from one that could be described by localized spins to the one with a decreased magnetic moment per cobalt ion and describable by delocalized spins. Finally, the electrochemical testing illustrated the improvement in the electrochemical per-

formance of the fluorinated electrode in terms of a higher galvanostatic capacity and a lower voltage hysteresis.

5. NANO-BIO MATERIALS FOR PREVENTIVE AND REGENERATIVE MEDICINE

HAp nanoparticles have been utilized in wide areas of research with a high potential for translation to applications in preventive, reconstructive and regenerative medicine. The design, synthesis and processing of HAp objects on the nano scale with optimal properties for application in this array of medical applications were our research goals for this project. Along with these aims, particles of nano-HAp coated with chitosan (Ch) or with Ch–PLGA polymer blend (HAp/Ch, HAp/Ch–PLGA) were designed and their suitability as drug carriers for intravenous administration proved. It was shown that after intravenous administration, HAp/Ch particles accumulated in the spleen and the liver, while HAp/Ch–PLGA particles accumulated in the lungs.[20] A new procedure for radiolabelling nano-HAp with ^{125}I was developed to determine the biodistribution and accumulation of the composite particles in different organs. Thus, the created nano-objects are highly prospective as carriers of medicaments to organs where their accumulation was detected. A wide range of synthetic steroidal heterocyclic derivatives with a five-membered or a six-membered ring were found feasible for use in the treatment of hormone-dependent cancers. The carriers based on nano-HAp coated with Ch–PLGA were found suitable as vehicles for the delivery of the steroid derivative 17β-hydroxy-17α-picolyl-androst-5-en-3β-yl-acetate (A). Nanosystems comprising A-loaded HAp/Ch–PLGA with different contents of A (7.5, 11.2 and 15 wt. %) were designed and their potential for activity toward lung cancer cells examined.[21] As the content of derivative A increased, so did the median value of the particle size distribution, with the particles containing 7.5, 11.2 and 15 wt.% A having the d_{50} values of 167, 168 and 231 nm, respectively. The cancer cell targeting potential of the particles was examined simultaneously on human lung cancer cells (A549) and human lung fibroblasts (MRC5) using the dye exclusion assay (DET) and the colorimetric test with the tetrazolium salt (MTT). All types of A-loaded HAp/Ch–PLGA particles showed an almost three times larger cytotoxicity towards cancerous cells than toward healthy ones. These results were in line with the initial aim of these studies, which was to design carriers for anticancer derivatives based on nano-HAp with a high toxicity to lung cancer and a low toxicity to healthy cells.

Steroid derivatives 3β-hydroxy-16-hydroxymino-androst-5-en-17-one ($C_{19}H_{27}NO_3$, B) and 3β,17β-dihydroxy-16-hydroxymino-androst-5-ene ($C_{19}H_{29}NO_3$, C) were further cancer inhibitors successfully entrapped in carriers composed of nano-HAp coated with ChOL.[22] The heterocyclic derivatives used, with three six-membered and one five-membered ring, differ only in the fact that derivative A has a keto group (>C=O) at the C17 position of the five-membered

cyclic ring, where B has an –OH group. ^{1}H-NMR and ^{13}C-NMR techniques confirmed that the structures of the synthesized derivatives B and C were intact after the entrapment inside the particles of nano-HAp coated with ChOL. Spherical particle morphologies, with the particle sizes of 80–150 and 100–240 nm, were obtained for B- and C-loaded HAp/ChOL, respectively (Fig. 8), while the contents of the derivatives B and C were 8.6 and 8.7 wt. %, respectively. The small difference in the structure of derivatives B and C resulted not only in different physicochemical properties of the two systems (B- *vs.* C-loaded HAp/ /ChOL), but also a difference in the activity towards the cancer cells and the healthy cells. C-loaded HAp/ChOL particles were particularly selective and they showed an almost six times greater cytotoxicity to breast cancer cells (MCF7 and MDA MB231) than to healthy cells (MRC5), according to the MTT test. Meanwhile, DET testing after 48 h of treatment with C-loaded HAp/ChOL particles resulted in a high viability of healthy cells (83 %), while the viability of breast cancer cells (MDA MB231) was the lowest (28 %).

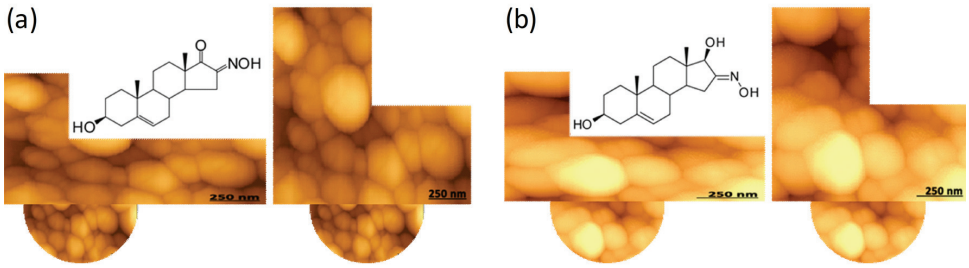

Fig. 8. Chitosan oligosaccharide lactate-coated hydroxyapatite nanoparticles (HAp/ChOL) as a vehicle for the delivery of steroid derivatives; a) 3β-hydroxy-16-hydroxymino-androst-5-en--17-one and b) 17β-dihydroxy-16-hydroxymino-androst-5-ene.

Reconstruction of bone defects with hybrid materials based on nano-HAp and bioresorbable polymers is commonly used in reconstructive medicine. After the hybrid material is applied to reconstruct a damaged bone, it is important to know how and in what way it affects distant organs. To answer this question, a mandibular bone reconstruction was performed *in vivo* with particles of PLGA--coated HAp (HAp, d_{50} = 75 nm; HAp/PLGA, d_{50} = 82 nm) and histopathological analysis of distant organs, kidney and liver parenchyma, was performed The liver and the kidneys were selected because products of the integration and degradation of the material are normally transported to them *via* body fluids. The reconstruction of the mandibular bone defect with HAp/PLGA resulted in an increase in the content of Ca and P in the newly created bone without pathological changes in the liver or the kidneys (Fig. 9).[23]

In addition to inorganic and inorganic–polymeric nanoparticles,[24] micro- and nano-polymer systems also represent a broad research field with a high pot-

ential for nanomedicine applications.[25] As part of this project, poly(ε-caprolactone) (PCL)-based microspheres were fabricated in a form suitable for achieving prolonged selenium nanoparticle (SeNP) release profiles.[26] These systems allowed for a slow and prolonged release of this particulate antimicrobial agent in physiological media and a fast release in adequate bacterial surroundings. Under the physiological conditions, at nearly neutral pH, a very slow release of SeNPs occurred (3 and 8 % SeNPs) after 660 days. On the other hand, the release in a medium supplemented with bacterial extract was 30 % after 49 days. The release of SeNPs from PCL microspheres with the diameter of 1–4 μm resulted in considerable antibacterial activity, particularly against the Gram-positive bacteria, *Staphylococcus aureus* and *Staphylococcus epidermidis*, which could be significant for reducing the inflammatory processes following a biomaterial implantation.

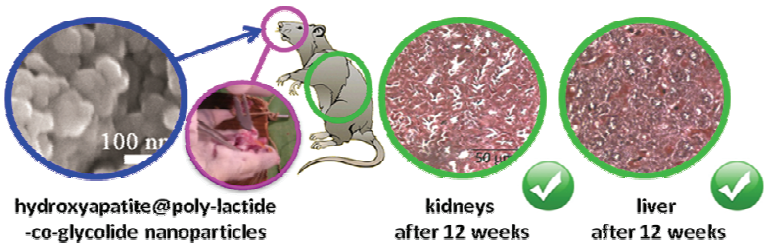

Fig. 9. Liver and kidney parenchyma after the reconstruction of mandibular bone defects with hydroxyapatite@poly-l-lactide-co-glycolide (HAp/PLGA) nanoparticles.

Cell scaffolds comprising Ch/PLGA were designed and shown to be suitable for incorporating gadolinium fluoride (Gd) nanoparticles as the T_1 contrast agent in MRI.[27] Cell scaffolds are generally used in cell transplantation as they provide a good mechanical support for the implanted cells. The controlled release of Gd from Gd–incorporated cell scaffolds allowed for the adequate activation of the MRI agent, which enabled the immune response of the implanted cells to be monitored. The Gd-incorporated Ch/PLGA cell scaffolds were composed of hollow spherical and ellipsoidal particles of 200–600 μm in diameter and a shell thickness of 50–80 μm. Most of the larger particles had several holes on their surface, which in some cases revealed complex interior cavities. The utility of Gd-incorporated Ch/PLGA scaffolds containing human mesenchymal stromal cells was successfully validated by MRI for 18 days *in vivo*.

Understanding the precise mechanisms of the action of nanoparticles is one of the prerequisites for enabling their rational design for preventive and regenerative biomedical applications. One of the studies had as its objective the delineation of the exact properties of calcium phosphate nanoparticles that are responsible for their exhibiting a moderate antibacterial activity.[28] This conceptually novel study proceeded by designing experimental conditions for testing nine sep-

arate particle properties and untangling one variable at a time as much as this was possible in a multivariable system where changes in each particle property affect to some degree other properties. The study demonstrated that a number of particle properties have simultaneous and synergistic effects on inhibiting bacterial growth and they included: *i*) nanoscopic size; *ii*) elevated intracellular free calcium levels due to nanoparticle solubility; *iii*) diffusivity and favourable electrostatic properties of the nanoparticle surface, primarily low net charge and high charge density; *iv*) the dynamics of perpetual exchange of ultrafine clusters across the particle/solution interface (Fig. 10). Nowhere less importantly, the study refuted the proposed parallel in the mechanism of action between calcium phosphate and zinc oxide, titanium oxide and other materials, the antibacterial activity of which is due to the activation of electronic transitions at defect sites induced by UV light.

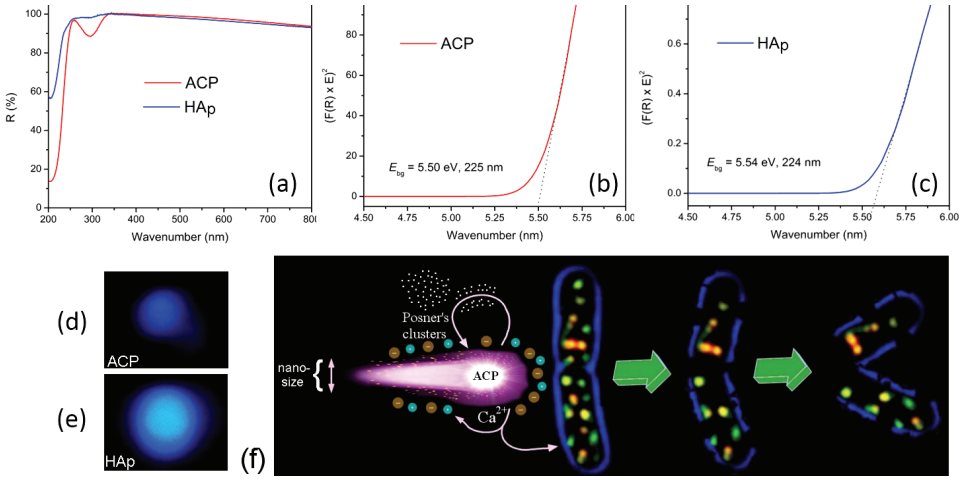

Fig. 10. UV–Vis diffuse reflectance spectra of ACP and HAp (a), along with the Kubelka–Munk curves from which the band gap energies were calculated (b, c), the luminescence photographs of ACP and HAp powders under 405 nm irradiation in the dark (d, e), and a scheme describing key particle properties acting as determinants of the antibacterial activity of CP nanoparticles in interaction with bacterial cells, including: *i*) nanoscopic size; *ii*) the release of calcium ions and elevation of the intracellular concentration of calcium; *iii*) diffusivity and low globally negative charge of a zwitterionic surface that minimizes the electrostatic barrier posed for the nanoparticle approaching the bacterial cell; *iv*) Posner's and similarly sized atomic clusters creating a rich and dynamic hydrodynamic environment surrounding the diffusive nanoparticles (f). (Reproduced with the permission of the American Institute of Physics).[28]

In late 2015, work began on a book the goal of which was to gather world-renowned experts from the field of nanomedicine and have them contribute with either their opinions as to whence and where to this field develops or up-to-date

reviews of their and their peers' work in this field. The book was eventually issued by Elsevier in 2018, with the title "Nanotechnologies in Preventive and Regenerative Medicine: An Emerging Big Picture",[29] containing the work of 58 different authors from five continents of the world. The book targeted versatile audiences, including academics, biotech and other industrial professionals, medical practitioners as well as students from numerous disciplines that intersect at the nanotechnology field. It provides an overview of state-of-the-art research in nanotechnologies for the early diagnosis and *in situ* monitoring of disease, for tissue engineering, for 3D printing, and for targeted and theranostic applications. It also provides the information important for the understanding of the biomolecule/nanosystems interface and the environmental fate of nanomaterials used in medicine. The book includes a chapter by Vranješ-Đurić and Ignjatović,[20] in which hybrids between radionuclides and nanoparticles are discussed from the viewpoints of their structure, fabrication, fate in the body and applications in imaging and targeted radiotherapy. The final chapter[30] by Uskoković and Uskoković took on the risky task of challenging some of the unequivocally accepted prospects in the field of medical nanotechnologies and questioning its paradigms and premises that rarely get questioned, if at all.

6. CONCLUSIONS

In the course of this report, we have provided a review of some of the central research achievements of the MODENAFUNA project for the years 2016 through 2019, when the project officially closed, after nine years of activity. The report gives an insight into the bibliographically most impactful Serbian national project on nanotechnologies executed within the aforementioned nine-year cycle. The project provided an outstanding and internationally recognized contribution to the synthesis, characterization and functional design of a number of materials systems, including pure and lantanide–doped hydroxyapatite, zinc oxides, sodium cobaltates, lithium iron pyrophosphates, carbon composites, titania nanotubes, lithium iron silicates and a number of polymeric systems. The project also provides a contribution meaningful for a number of different applications, ranging from fundamental physicochemical to environmental to pharmaceutical to medical.

The realization of this project did not proceed without difficulties. The key equipment was not delivered on time or not at all, the direct material costs were not as per the originally approved budget, and so on. Due to all these setbacks, the room for the creation of an innovative spin-off space lacked, delaying the translation of these technologies to the applicative domain. On a more positive note, all the young researchers involved within this project successfully completed their doctoral studies and continued to work at the Institute, thus preserving the critical creative force for the continued excellence in research on nanotechnologies. The realization of the project also defied the prevailing opinion in

Serbia that researchers in the retirement age are incapable of running successful research programs, given that the principal investigator of this project was between 67 and 76 years of age during its execution and was funded only for the first four months out of its nine-year duration.

Finally, it is hoped that the findings that arising from this project will provide the basis for future research on nanotechnologies by this group of authors and their collaborators. It is equally hoped that they will serve as an inspiration and an incentive to other research groups in Serbia and countries that share its unfortunate past and lack of economic privilege on the continental and the global scales that despite the hardships, truly excellent science that resonates beyond the national boundaries is still possible.

SUPPLEMENTARY MATERIAL

Additional data are available electronically at the pages of journal website: https://www.shd-pub.org.rs/index.php/JSCS/index, or from the corresponding author on request.

Acknowledgements. Funds for the realization of this work are provided by the Ministry of Education, Science and Technological Development of the Republic of Serbia; Agreement on the realization and financing of scientific research work of the Institute of Technical Sciences of SASA in 2020 (Record number: 451-03-68/2020-14/200175) and under Project No. III45004, "Molecular designing of nanoparticles with controlled morphological and physicochemical characteristics and functional materials based on them". Collaborative research performed in the United States was supported by the NIH R00-DE021416 grant.

И З В О Д

ОД МОЛЕКУЛА ДО НАНОЧЕСТИЦА И ФУНКЦИОНАЛНИХ МАТЕРИЈАЛА

НЕНАД Л. ИГЊАТОВИЋ[1], СМИЉА МАРКОВИЋ[1], ДРАГАНА ЈУГОВИЋ[1], ВУК УСКОКОВИЋ[2] и ДРАГАН П. УСКОКОВИЋ[1]

[1]Институт техничких наука Српске академије наука и уметности, Кнеза Михаила 35/4, 11000 Београд и [1]Department of Mechanical and Aerospace Engineering, University of California Irvine, Engineering Gateway 4200, Irvine, 92697, CA, USA

Функционални материјали држе чврсту позицију на челу науке и инжењерства материјала у 21. веку. "Молекуларно дизајнирање наночестица са контролисаним морфолошким и физичко–хемијским својствима и функционалних материјала на њиховој бази" (MODENAFUNA) је назив пројекта финансираног од стране Министарства просвете, науке и технолошког развоја Републике Србије и оствареног између 2011. и 2019. године у програму интегралних интердисциплинарних истраживања, а у оквиру научне области нови материјали и нанонауке. Програм је реализован кроз активности организоване у пет међусобно повезаних тема: 1) од молекула до наночестица, 2) напредна керамика са побољшаним функционалним својствима, 3) електродни материјали за литијум-јонске батерије, 4) нано-калцијум-фосфат у превентивној и регенеративној медицини, 5) биоразградиве микро- и наночестице за контролисану испоруку лекова. Овде приложен извештај даје увид у овај библиографски најутицајнији српски национални пројекат на тему нанотехнологија реализован у оквиру датог деветогодишњег периода. У главном делу су описани резултати постигнути у последње три године (2016–2019), док додатак представља суму резултата остварених у целокупном периоду од 2011. до 2019. Пројекат је дао изузетан и међународно признат допринос синтези,

карактеризацији и функционалном дизајну бројних материјала, укључујући чист хидроксиапатит и хидроксиапатит допиран ретким земљама, оксиде цинка, натријум-кобалтате, литијум–гвожђе-пирофосфате, угљеничне композите, титан-оксидне наноцеви, литијум–гвожђе-силикате и низ полимерних система. Сагледан у оквирима науке о материјалима у некада развијеној европској земљи која је претрпела брзи економски пад, кашњење у технолошком напретку и одлив мозгова, посебно током деведесетих година прошог века, овај преглед може бити занимљив како националној тако и међународној публици.

(Примљено 20. априла, прихваћено 15. јуна 2020)

REFERENCES

1. N. L. Ignjatović, S. Marković, D. Jugović, D. P. Uskoković, *J. Serb. Chem. Soc.* **82** (2017) 607 (https://doi.org/10.2298/JSC1612070011I)
2. J. Choi, S. Park, Z. Stojanović, H. S. Han, J. Lee, H. K. Seok, D. Uskoković, K. H. Lee, *Langmuir* **29** (2013) 15698 (https://doi.org/10.1021/la403888f)
3. Z. Stojanović, M. Otoničar, J. Lee, M. M. Stevanović, M. P. Hwang, K. H. Lee, J. Choi, D. Uskoković, *Colloids Surfaces, B* **109** (2013) 236 (https://doi.org/10.1016/j.colsurfb.2013.03.053)
4. M. Vukomanović, S. D. Škapin, B. Jančar, T. Maksin, N. Ignjatović, V. Uskoković, D. Uskoković, *Colloids Surfaces, B* **82** (2011) 404 (https://doi.org/10.1016/j.colsurfb.2010.09.011)
5. M. Stevanović, V. Uskoković, M. Filipović, S. D. Škapin, D. Uskoković, *ACS Appl. Mater. Interfaces* **5** (2013) 9034 (http://dx.doi.org/10.1021/am402237g)
6. N. L. Ignjatović, L. Mančić, M. Vuković, Z. Stojanović, M. G. Nikolić, S. Škapin, S. Jovanović, L. Veselinović, V. Uskoković, S. Lazić, S. Marković, M. M. Lazarević, D. P. Uskoković, *Sci. Rep.* **9** (2019) 16305 (https://doi.org/10.1038/s41598-019-52885-0)
7. J. C. Hemminger, J. Sarrao, G. Crabtree, G. Flemming, M. Ratner, *Challenges at the Frontiers of Matter and Energy: Transformative Opportunities for Discovery Science*, U.S. Department of Energy, Washington, DC, 2015 (https://doi.org/10.2172/1283188)
8. V. Uskoković, *Cryst. Growth Des.* **19** (2019) 4340 (https://doi.org/10.1021/acs.cgd.9b00061)
9. V. Uskoković, S. Marković, L. Veselinović, S. Škapin, N. Ignjatović, D. P. Uskoković, *Phys. Chem. Chem. Phys.* **20** (2018) 29221 (https://doi.org/10.1039/C8CP06460A)
10. S. Marković, A. Stanković, J. Dostanić, L. Veselinović, L. Mančić, S. D. Škapin, G. Dražič, I. Janković-Častvan, D. Uskoković, *RSC Adv.* **7** (2017) 42725 (https://doi.org/10.1039/C7RA06895F)
11. S. Marković, V. Rajić, A. Stanković, L. Veselinović, J. Belošević-Čavor, K. Batalović, N. Abazović, S. D. Škapin, D. Uskoković, *Sol. Energy* **127** (2016) 124 (http://dx.doi.org/10.1016/j.solener.2016.01.026)
12. S. Marković, I. Stojković Simatović, S. Ahmetović, L. Veselinović, S. Stojadinović, V. Rac, S. D. Škapin, D. Bajuk Bogdanović, I. Janković Častvan, D. Uskoković, *RSC Adv.* **9** (2019) 17165 (https://doi.org/10.1039/C9RA02553G)
13. V. N. Ivanovski, J. Belošević-Cavor, V. Rajić, A. Umićević, S. Marković, V. Kusigerski, M. Mitrić, V. Koteski, *J. Appl. Phys.* **126** (2019) 125703 (https://doi.org/10.1063/1.5095837)
14. M. Bratić, D. Jugović, M. Mitrić, N. Cvjetićanin, *J. Alloys Compd.* **712** (2017) 90 (https://doi.org/10.1016/j.jallcom.2017.04.065)

15. M. D. Milović, D. D. Vasić Anićijević, D. Jugović, V. J. Anićijević, L. Veselinović, M. Mitrić, D. Uskoković, *Solid State Sci.* **87** (2019) 81 (https://doi.org/10.1016/j.solidstatesciences.2018.11.008)
16. D. Jugović, M. Mitrić, M. Milović, V. N. Ivanovski, S. Škapin, B. Dojčinović, D. Uskoković, *J. Alloys Compd.* **786** (2019) 912 (https://doi.org/10.1016/j.jallcom.2019.01.392)
17. D. Jugović, M. Mitrić, M. Milović, N. Cvjetićanin, B. Jokić, A. Umićević, D. Uskoković, *Ceram. Int.* **43** (2017) 3224 (https://doi.org/10.1016/j.ceramint.2016.11.149)
18. M. Milović, D. Jugović, N. Cvjetićanin, D. Uskoković, A. S. Milošević, Z. S. Popović, F. R. Vukajlović, *J. Power Sources* **241** (2013) 70 (http://dx.doi.org/10.1016/j.jpowsour.2013.04.109)
19. D. Jugović, M. Milović, M. Popović, V. Kusigerski, S. Škapin, Z. Rakočević, M. Mitrić, *J. Alloys Compd.* **774** (2019) 30 (https://doi.org/10.1016/j.jallcom.2018.09.372)
20. T.-J. Wu, H.-Y. Chiu, J. Yu, M. P. Cautela, B. Sarmento, J. das Neves, C. Catala, N. Pazos-Perez, L. Guerrini, R. A. Alvarez-Puebla, S. Vranješ-Đurić, N. L. Ignjatović, in *Nanotechnologies in Preventive and Regenerative Medicine*, V. Uskoković, D. P. Uskoković (Eds.), Elsevier, Amsterdam, 2018, p. 1 (https://doi.org/10.1016/B978-0-323-48063-5.00001-0)
21. N. L. Ignjatović, K. M. Penov-Gaši, J. J. Ajduković, V. V. Kojić, S. B. Marković, D. P. Uskoković, *Mater. Sci. Eng., C* **89** (2018) 371 (https://doi.org/10.1016/j.msec.2018.04.028)
22. N. L. Ignjatović, M. Sakač, I. Kuzminac, V. Kojić, S. Marković, D. Vasiljević-Radović, V. M. Wu, V. Uskoković, D. P. Uskoković, *J. Mater. Chem., B* **6** (2018) 6957 (https://doi.org/10.1039/C8TB01995A)
23. N. L. Ignjatovic, R. Jankovic, V. Uskokovic, D. P. Uskokovic, *Toxicol. Res. (Camb).* **8** (2019) 287 (https://doi.org/10.1039/c9tx00007k)
24. M. Stevanović, M. J. Lukić, A. Stanković, N. Filipović, M. Kuzmanović, Ž. Janićijević, in *Materials for Biomedical Engineering*, V. Grumezescu, A. Grumezescu (Eds.), Elsevier, Amsterdam, 2019, p. 1 (https://doi.org/10.1016/B978-0-08-102814-8.00001-9)
25. M. Stevanović, in *Nanostructures for Drug Delivery*, E. Andronescu, A. Grumezescu (Eds.), Elsevier, Amsterdam, 2017, p. 355 (https://doi.org/10.1016/B978-0-323-46143-6.00011-7)
26. N. Filipović, L. Veselinović, S. Ražić, S. Jeremić, M. Filipič, B. Žegura, S. Tomić, M. Čolić, M. Stevanović, *Mater. Sci. Eng., C* **96** (2019) 776 (https://doi.org/10.1016/j.msec.2018.11.073)
27. V. Catanzaro, G. Digilio, F. Capuana, S. Padovan, J. C. Cutrin, F. Carniato, S. Porta, C. Grange, N. Filipović, M. Stevanović, *J. Funct. Biomater.* **10** (2019) 28 (https://doi.org/10.3390/jfb10030028)
28. V. Uskoković, S. Tang, M. G. Nikolić, S. Marković, V. M. Wu, *Biointerphases* **14** (2019) 031001 (https://doi.org/10.1116/1.5090396)
29. V. Uskoković, D. P. Uskoković, in *Nanotechnologies in preventive and regenerative medicine*, V. Uskoković, D. P. Uskoković (Eds.), Elsevier, Amsterdam, 2018, p. xxi (https://doi.org/10.1016/C2016-0-00418-7)
30. V. Uskoković, D. P. Uskoković, in *Nanotechnologies in preventive and regenerative medicine* ,V. Uskoković, D. Uskoković (Eds.), Elsevier, Amsterdam, 2018, p. 513 (https://doi.org/10.1016/B978-0-323-48063-5.00012-5).